ELSEVIER

Ultramicroscopy 82 (2000) 1–9

ultramicroscopy

www.elsevier.nl/locate/ultramic

A cantilever array-based artificial nose

M.K. Baller[a,b], H.P. Lang[a,b,*], J. Fritz[a,b], Ch. Gerber[a], J.K. Gimzewski[a], U. Drechsler[c], H. Rothuizen[c], M. Despont[c], P. Vettiger[c], F.M. Battiston[d], J.P. Ramseyer[d], P. Fornaro[d], E. Meyer[d], H.-J. Güntherodt[d]

[a]*IBM Research, Zurich Research Laboratory, Nanoscale Science Dept., Säumerstrasse 4, CH-8803 Rüschlikon, Switzerland*
[b]*Institute of Physics, University of Basel, Klingelbergstrasse 82, CH-4056 Basel, Switzerland*
[c]*IBM Research, Zurich Research Laboratory, Micromechanics Dept., Säumerstrasse 4, CH-8803 Rüschlikon, Switzerland*
[d]*Institute of Physics, University of Basel, Klingelbergstrasse 82, CH-4056 Basel, Switzerland*

Received 31 May 1999; received in revised form 17 August 1999

Abstract

We present quantitative and qualitative detection of analyte vapors using a microfabricated silicon cantilever array. To observe transduction of physical and chemical processes into nanomechanical motion of the cantilever, swelling of a polymer layer on the cantilever is monitored during exposure to the analyte. This motion is tracked by a beam-deflection technique using a time multiplexing scheme. The response pattern of eight cantilevers is analyzed via principal component analysis (PCA) and artificial neural network (ANN) techniques, which facilitates the application of the device as an artificial chemical nose. Analytes tested comprise chemical solvents, a homologous series of primary alcohols, and natural flavors. First differential measurements of surface stress change due to protein adsorption on a cantilever array are shown using a liquid cell.

PACS: 07.07.Df; 07.79. − v; 61.16.Ch; 07.10.Cm

Keywords: Artificial nose; Micromechanics; Chemical sensors; Protein adsorption

1. Introduction

Recently, increasing efforts have been put into the development of cantilever-based sensors for the detection of physical phenomena and chemical reactions. Miniaturized sensors show fast responses, high sensitivity, and are suitable for mass production. Their main application fields are quality and process control, disposable diagnostic biosensing for medical analysis, fragrance design, oenology, and as sensing devices for gaseous analytes, e.g. process gases or solvent vapors.

The application of single-cantilever sensors to determine quantities below the detection limits of equivalent "classical" methods has been demonstrated in the literature: Gimzewski et al. have shown that catalytic processes can be observed with picojoule sensitivity in calorimetry [1]. The cantilever method allows the study of solid–solid

* Corresponding author. Tel.: + 41-1-724-8929; fax: + 41-1-724-8964.

E-mail address: hpl@zurich.ibm.com (H.P. Lang)

0304-3991/00/$ - see front matter
PII: S0304-3991(99)00123-0

phase transitions of alkanes [2,3] using minute quantities of material in the picogram range. Formation enthalpies of small Sn metallic clusters have been determined in the gas phase using microcantilevers [4]. Cantilever sensors have been applied for photothermal spectroscopy [5], surface stress detection [6–8], infrared radiation detection [9], mass change detection [10,11], photothermal sensors [12–14] and thermogravimetry [15]. Cantilever sensors can be operated in liquids to observe such processes as protein adsorption [16].

The sensor presented is based on a microfabricated array of silicon cantilevers. Each of the cantilevers is functionalized by coating it with a specific sensor layer to transduce a physical process or a chemical reaction into a nanomechanical response. Such arrays allow use of some cantilevers as reference sensors (differential measurements) [17–19]. Here, we mainly take advantage of the swelling effect of polymers upon exposure to gaseous analytes. The kinetics of the swelling process is related to the vapor pressure and the solubility characteristics of the analyte in the polymers. In addition, effects related to heat transfer or mass change can be evaluated for analyte detection.

2. Experimental

2.1. Sample chamber setup

Sensor parallelism is a key prerequisite for applications requiring a high degree of complexity and selectivity [20–24]. Our sensor array chip (Fig. 1) comprises eight linearly arranged cantilever-type sensors (length: 500 μm, width: 100 μm, thickness: 1 μm, pitch: 250 μm), which can be sensitized individually for various detection purposes. This array is housed in a sample chamber made of aluminum (volume: 6 cm^3) with analyte inlet and outlet as well as windows for cantilever deflection readout (Fig. 2). Cantilever deflection is measured via incident light beams from eight individual light sources having the same pitch as the cantilevers (vertical cavity surface emitting lasers (VCSELs) optical power: up to 2 mW, wavelength: 760 nm, single mode emitters, CSEM Zürich, Switzerland). The identical pitch of light sources and cantilevers facilitates the optical readout of sensors via beam deflection. Optics consist of a doublet of achromatic lenses providing a 1 : 1 projection. The light is reflected off the cantilever apex and collected by a linear position-sensitive detector (PSD). To simplify device construction, a time-multiplexing

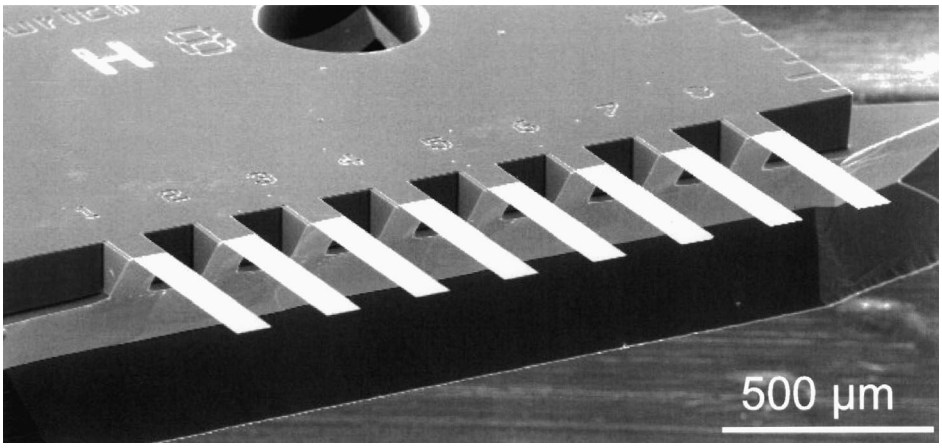

Fig. 1. Scanning electron microscopy image of a microfabricated cantilever sensor array prior to deposition of sensor coatings. The array was produced from silicon by combined dry and wet etching techniques in the Micromechanics department at the IBM Zurich Research Laboratory. Cantilever length: 500 μm, thickness: 1 μm, width: 100 μm. Typical spring constant: 0.02 N m^{-1}.

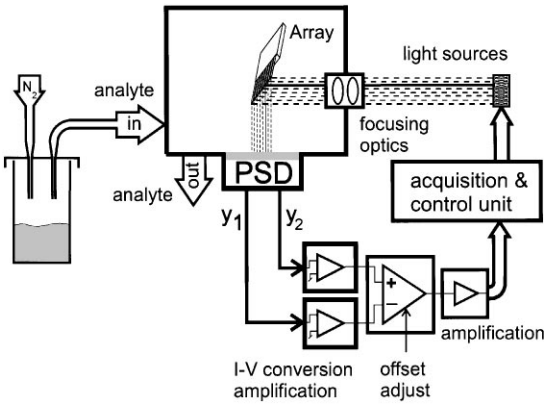

Fig. 2. Schematic setup of sample chamber with analyte inlet and outlet, cantilever deflection readout electronics and control. The acquisition and control unit sequentially switches the light sources on and off via a time-multiplexing scheme (40 ms for each cantilever). The laser light ($\lambda = 760$ nm) is directed via focusing optics onto the apex of the cantilevers of the array, then reflected and collected by a linear position sensitive detector (PSD). The photocurrents from opposing electrodes are converted into voltages. The voltage difference is adjusted by an offset to allow optimal amplification and fed into the data acquisition and control unit. Data processing is performed off-line on a personal computer.

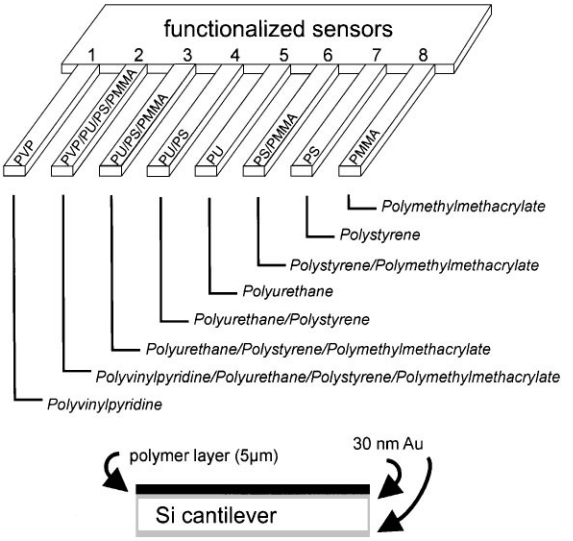

Fig. 3. Schematic view of a cantilever array with polymer coatings used for the eight cantilevers of the sensor array. PVP = polyvinylpyridine, PU = polyurethane, PS = polystyrene, PMMA = polymethylmethacrylate. Schematic cross section of a coated cantilever.

scheme [17,18] is applied by switching on and off individual light sources to illuminate only one cantilever apex at a time and to provide an electrical signal at the PSD for each cantilever deflection three times per second. The y position of the light spots on the PSD depends directly on the difference of photocurrents from opposing electrodes. The photocurrents are converted into voltages using transimpedance amplifiers, and the voltage difference is transmitted to a data acquisition and control unit. This so-called nanotechnology olfactory sensors (NOSE) system [25] consists of modular units, which can be expanded by further sensor arrays.

2.2. Cantilever sensor coatings

Cantilever sensor arrays were coated with 30 nm of gold by electron beam evaporation. Polymers were spray-coated onto one side of the cantilevers to form a homogeneous layer of ≈ 5 μm thickness (Fig. 3). Commercially available polymers were dissolved in toluene or ethanol (concentrations for all solutions: 5 mg/ml).

2.3. Data acquisition and analysis

An automated gas handling system [25] is used for programmed exposure of the sensor array to various gaseous analytes. Gas flows are adjusted in the range of 2–100 ml/min by software-driven commercial digital mass flow controllers (Bronkhorst, The Netherlands). By means of two mass-flow controllers it is possible to mix carrier gas (dry nitrogen, purity 99.999990%) with well-defined amounts of analyte. Two-hundred microliter of each analyte was filled into 4-ml vials closed by a septum. Vapor from the head space was injected into the chamber via the gas handling system (Fig. 2).

The sensitized cantilever array is exposed to the analyte for 10 s. Then, the cantilever response is measured for 2 min while being purged with nitrogen. To reduce the amount of data the normalized signal amplitude is evaluated for each cantilever at

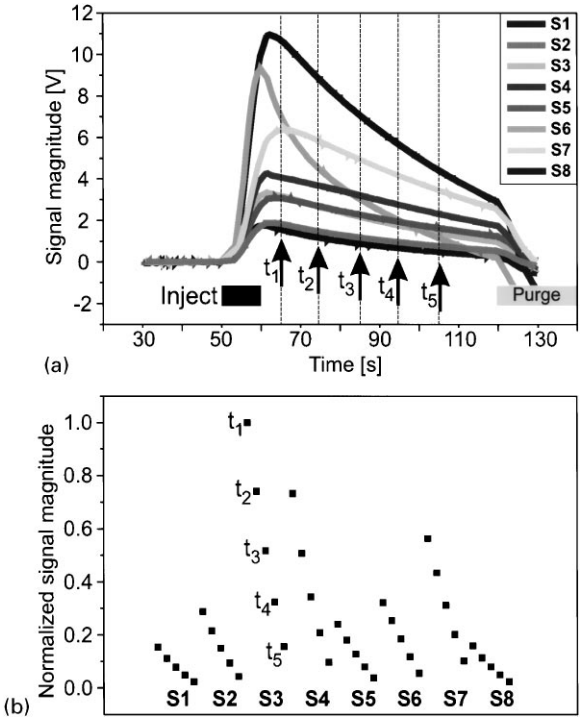

Fig. 4. (a) Reaction traces from eight polymer-coated cantilevers upon injection of ethanol for 10 s. Signal magnitudes at five points in time t_1–t_5 are extracted. These data points sufficiently characterize the analyte desorption process. (b) Normalizing these five response magnitudes from all eight cantilevers (S1–S8) yields a fingerprint pattern of the analyte suitable for further analysis via principal component analysis and neural network techniques.

five equidistant points in time (Fig. 4). This fingerprint information (five points for eight cantilevers = 40 parameters) reflects the analyte desorption characteristics, which were found to result in a better separation of the analytes compared to the adsorption characteristics and the maximum amplitudes of the sensor response. The fingerprint is analyzed by a commercial principal component analysis (PCA) software package (MVSP, multivariate statistical package, version 3.0, Kovach Computing Services, UK). PCA extracts most-dominant deviations in responses for various analytes. The largest differences in signal amplitudes of the fingerprint patterns are plotted in a two-dimensional graph. The axes refer to projections of the multidimensional datasets into two dimensions (principal components). This procedure is aimed at maximum distinction performance between analytes, i.e. several measurements of the same analyte should yield a cluster in principal component space, whereas measurements of different analytes should yield well-separated clusters.

For more complex measurements, e.g. to analyze multicomponent mixtures of gaseous analytes such as natural flavors, a different strategy involving artificial neural networks (ANN) is pursued. Whereas PCA extracts most-dominant differences in the fingerprint pattern, neural network analysis considers all components of the fingerprint. Using several training sets for each analyte, the ANN software package (e.g. Neuroshell Classifier, Version 2.0, Ward Systems Group Inc., USA) can "learn" the corresponding fingerprint pattern to identify the analytes.

2.4. Stress measurements in liquids

To measure stress-related cantilever bending in liquid environment we use a setup based on a modified commercial atomic force microscope head and liquid cell (Digital Instruments, Santa Barbara, CA, USA), which can be modified for current flow experiments. The volume of the liquid cell (≈ 800 μl) can be injected or exchanged with a micropipette. For simplicity we use a cantilever array of two gold-coated Si cantilevers (cantilever length: 500 μm, width: 100 μm, thickness: 1 μm, pitch: 500 μm, thickness of evaporated gold layer: 30 nm). This system can easily be upgraded to operation with multiple cantilever arrays. Utilizing a similar readout technique based on VCSEL light sources and PSD as described above, cantilever bending can be observed individually for each cantilever.

The gold surface of one cantilever was blocked for protein adsorption by 11-(pentaethylene glycol)undecan-1-thiol (PEG5 thiol, courtesy of Fadhil Kamounah, University of Copenhagen, Denmark). The other was functionalized for adsorption by hydrophobic hexadecanthiol (HDT, Fluka Chemicals, Buchs, Switzerland, further purified by column chromatography). Adsorption

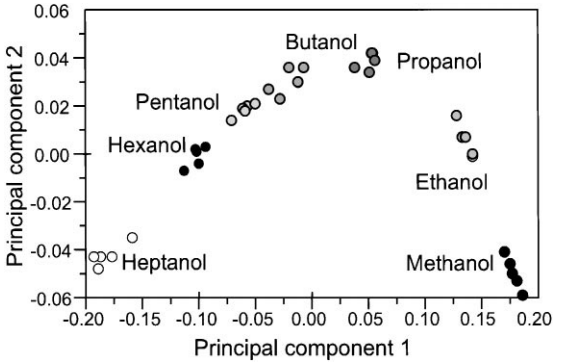

Fig. 5. Principal component analysis (PCA) of primary alcohols in a two-dimensional representation in principal component space. Analytes form clearly separated clusters ordered according to their molecular weight.

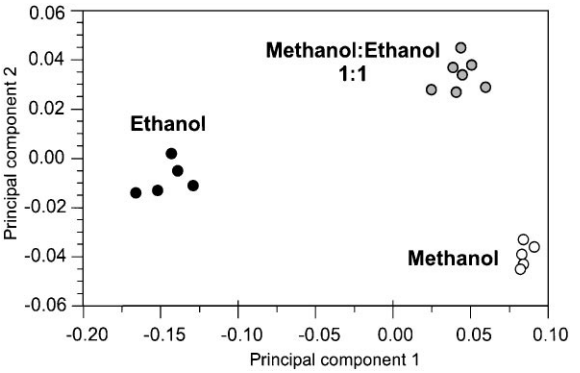

Fig. 6. PCA of methanol, ethanol, and a 1 : 1 mixture of both alcohols showing distinct clusters.

of bovine serum albumine (BSA, 1 mg/ml, Sigma–Aldrich Chemicals, Buchs, Switzerland, in phosphate-buffered saline, PBS, pH 7.4, Fluka Chemicals, Buchs, Switzerland) on HDT and the block of BSA adsorption by PEG5 were checked by ellipsometry (data not shown).

3. Results and discussion

3.1. Homologous series of primary alcohols

To demonstrate the analyte recognition capability of our NOSE device, a homologous series of primary alcohols from methanol to heptanol (Fluka Chemicals, puriss., p.a. grade, Buchs, Switzerland) was investigated. Octanol and higher alcohols are not considered due to the relatively low vapor pressures and thus long desorption times. As an example the cantilever responses for ethanol are displayed in Fig. 4a.

All analytes were measured five times in random order to exclude systematic influences. The results were found to be reproducible. This set of fingerprints was analyzed using PCA based on the procedure described in Fig. 4. The result is shown in Fig. 5. The five measurements of each analyte show distinct clusters in principal component space and allow unambiguous identification of analytes.

3.2. Mixture of alcohols

We extended the previous investigations to study how a mixture of alcohols is characterized by PCA methods. For this purpose a mixture of 100 μl of methanol and 100 μl of ethanol was put into a vial for measurement. The principal components evaluated based on seven fingerprint data sets showed clear clustering (Fig. 6). Special care had to be taken concerning the amount of vapor extracted in the head space of the vial in order not to influence the composition of the vapor mixture due to the difference in vapor pressures of methanol and ethanol. Using PCA it is possible to distinguish among different mixtures of analytes provided that these mixtures have been previously characterized by PCA. It is difficult to determine the mixing ratio of individual analytes directly from the cluster positions of mixture constituents in the PCA plot, because analyte desorption kinetics of analyte mixtures do not depend on the mixing ratio in a clearly predictable way.

3.3. Solvents

Polar and unpolar solvents such as water, ethanol, methanol, 1-propanol, 2-propanol, acetone, dichloro-methane, toluene, and heptane are widely used in chemical and technological production processes. To demonstrate the separation selectivity of our NOSE device we investigated

vapor samples of the above-mentioned solvents using 100 μl of analyte in vials as described above. Fig. 7 clearly shows clustering for the analytes tested, i.e. successful identification and selectivity. Further applications may be settled in the field of quality and purity control of solvents in production lines.

3.4. Natural flavors

Natural flavors designed to give bakery products a special taste are complex mixtures of various components, mainly water and 1,2-propanediol, in some cases ethanol, besides characteristic flavor ingredients. Typical examples of such bakery flavors are bitter almond (BA), cherry (CH), orange (OR), artificial rum (RU), vanilla (VA) and lemon (LE). Such analytes are difficult to separate by PCA, because similar ratios of the major constituents of these mixtures are present in all analytes, in particular water and 1,2-propanediol. For this reason ANN techniques were applied, taking into account all parameters from the fingerprint data sets. For each analyte, seven independent measurements were first recorded and fed as training sets into an ANN. Then, after this "learning" process, the success of recognition of another independent data set was determined. As can be seen in Table 1 all analytes were identified, five of which with a probability close to 1. Only the artificial rum sample has a lower identification probability of 0.728, but its identification probability could be increased significantly if more training sets for analytes were used.

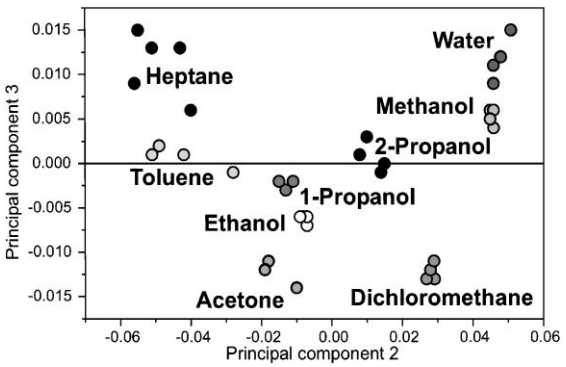

Fig. 7. PCA of various commonly used solvents.

3.5. Quantitative measurements

Fig. 8 shows quantitative measurements of 1-propanol concentrations ranging from 500 to 1000 ppm in steps of 100 ppm. This data was produced by adjusting the gas flow through the analyte vial in discrete steps using the gas handling system. The sensitivity is ≈ 30 ppm μm^{-1} deflection.

At the moment, the sensitivity-limiting factors in our system are the flow rates imposed by the gas handling system and the chamber volume, but not the cantilever deflection measurement

Table 1
Neural network analysis of natural flavors (*Note*: BA = bitter almond, CH = cherry, OR = orange, RU = artificial rum, VA = vanilla, LE = lemon. "Actual" signifies the actual species of analyte, "classified as" means the assignment by the neural network software based on a discrimination probability of at least 0.5. Numbers indicate identification probabilities. All analytes have been identified correctly (bold numbers). For most analytes the identification probability is close to 1, except for RU, which was identified with a probability of 0.728 only. For each analyte, seven training sets and one test set were used. The neural network was composed of five input and 15 hidden neurons.)

Test	Actual	Classified as	BA	CH	OR	RU	VA	LE
1	BA	BA	**0.993**	0.001	0.000	0.000	0.000	0.005
2	CH	CH	0.001	**0.923**	0.069	0.005	0.002	10.000
3	OR	OR	0.000	0.026	**0.974**	0.000	0.000	0.000
4	RU	RU	0.000	0.272	0.001	**0.662**	0.054	0.011
5	VA	VA	0.000	0.000	0.000	0.000	**0.994**	0.006
6	LE	LE	0.000	0.000	0.000	0.020	0.000	**0.980**

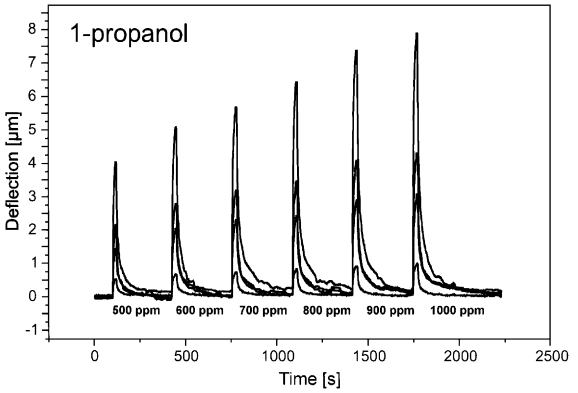

Fig. 8. Quantitative measurement of various concentrations of 1-propanol. For clarity, only four of the eight traces of cantilever motions are reproduced. Analyte injection time: 10 s, purging time (N_2): 6 min.

and the sensitivity of the sensor layer. A reduction of the chamber volume will increase the mass sensitivity and reduce response times. Measurement statistics can be enhanced using an autosampler instead of the gas handling system. Taking these improvements into account, estimated detection levels are expected to be well below 1 ppm.

3.6. Protein adsorption on a cantilever

An advantage of Si cantilever sensors is that they can be operated in different environments such as air, vacuum, or liquids. Especially operation in liquids introduces the possibility of using functionalized cantilevers as biosensors. The first application of Si cantilevers as resonant mass sensors was a biomass-monitoring device for living cells [26]. Further experiments are reported, where cells have been grown on cantilever surfaces and static deflections were measured due to cellular activity [27]. Other applications in liquids include surface stress measurements of electrochemical processes [28,29] and of adsorption of proteins on the cantilever surface [16,30]. Another type of experiments with biomolecules attempts to use Si cantilevers to monitor molecular recognition, for example of antibody–antigen interaction or DNA hybridization. The use of cantilevers allows molecular recognition to be transduced directly into a nanomechanical response.

The major disadvantage of surface stress measurements in liquids reported up to now is that experiments were performed without a reference cantilever. Using two or more cantilevers of a single array in parallel allows one of the cantilevers to be operated as a reference sensor. This is especially important for measuring the static deflection of cantilevers in liquids, because small changes of pH, ion concentration, refractive index, temperature, or even the quality and treatment of the cantilever surface can influence dramatically the deflection signal. For example, a change of the refractive index can mimic a deflection signal several tens of nanometers in magnitude. These artifacts can be cancelled out by measuring the differential signal between two sensors, an inert reference sensor and a specifically sensitized sensor.

Such a differential measurement is shown in Fig. 9. The liquid cell with two sensors in parallel was flushed with buffer, then with BSA, and again with buffer while recording the deflection signal of the two cantilevers. The raw data (Fig. 9a) shows turbulences due to injection of the liquid, thermal equilibration after injection for 10 min or more, and wave-like changes of the deflection signal due to a change of room temperature. In contrast, the differential signal (Fig. 9b) compensates for such thermal effects and most of the turbulences. Without thermal stabilization, it shows only a slight drift of about 5 nm h^{-1}. The gold surface of one sensor was covered by an alkylthiol and the other sensor by a PEG5 thiol. BSA adsorbs only on the hydrophobic surface of the alkylthiol sensors. PEG is known to block almost completely the adsorption of proteins such as BSA or antibodies on surfaces [31]. As BSA adsorbs to the same extent on the Si surfaces of both cantilevers, this adsorption process does not contribute to the differential signal.

The measured deflection is of the order of 25 nm and corresponds to a bending of the alkylthiol cantilever away from its gold surface. That is, the protein layer causes a compressive stress of about 0.006 N m^{-1}, as can be calculated with Stoney's formula [8]. Thereby the stress of the unordered physisorbed protein layer on top of the HDT is more than one order of magnitude smaller than the typical stress of about 0.2 N m^{-1} related to the self-assembly of thiols on gold. The adsorption of

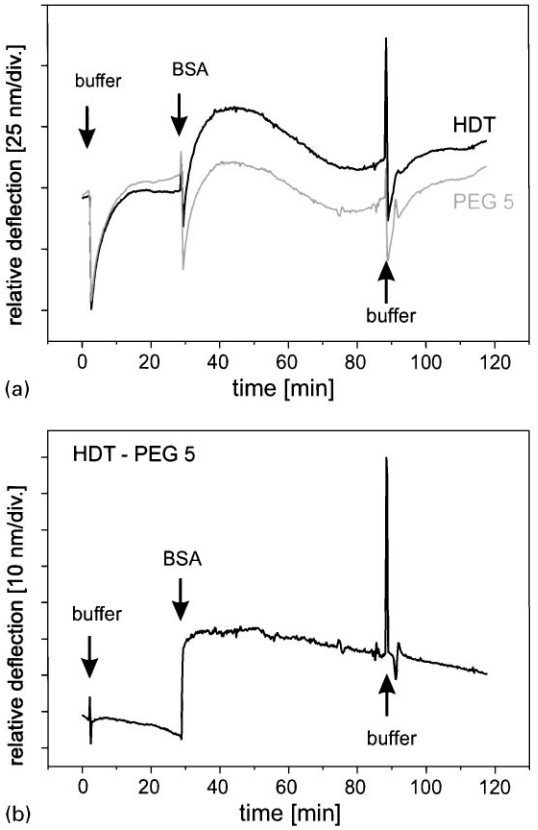

Fig. 9. (a) Deflection traces of HDT (black) and PEG 5-functionalized (grey) cantilevers on injection of BSA (raw data). The wavy behavior of the curves is due to thermal influences. (b) Difference in responses of HDT and PEG 5-covered cantilevers. Adsorption of BSA on the HDT surface is clearly observed (increase in deflection). Injection of buffer solution does not change the deflection any further. Peaks are due to the injection process (indicated by arrows).

the proteins on the hydrophobic surface occurs within a few minutes. Up to now, all adsorption measurements of various thiols and proteins on functionalized and non-functionalized surfaces show a compressive stress, that is, the cantilevers bend away from the surface on which the molecules adsorb [8].

4. Conclusion

In conclusion, we have demonstrated that a micromechanical array of cantilevers can be used as a selective and quantitative chemical sensor (artificial nose). It can be employed to create fingerprints of analytes. Its major advantages are the capability to use reference sensors for differential measurements that compensate for superimposed disturbances. Likewise, calibration offsets originating from misalignment or refractive-index changes by operation in liquids or gases can be corrected. As examples, quantitative and qualitative analyte detection and identification were demonstrated by covering the cantilevers with a system of various polymers and polymer blends. The cantilever deflection caused by a swelling of the polymer layers upon exposure to gaseous analytes was used to create fingerprints for PCA and ANN recognition techniques. Successful identification of a series of primary alcohols, commonly used solvents, and flavors for bakery products has been demonstrated.

The device is designed to operate in various media such as ambient air, vacuum, gases, and liquids. First results of sensor array operation in liquids have been shown, such as protein adsorption on cantilevers in fluids. The micromechanical design of the sensors implies short response times and high sensitivity over a wide range of operating temperatures, and they can be integrated seamlessly into microelectronic devices.

Acknowledgements

We thank P.F. Seidler and P. Guéret for helpful discussions as well as their support. We acknowledge support from E. Delamarche and A. Bernard, IBM Zurich Research Laboratory. This work is partially funded by the Swiss National Science Foundation priority program MINAST (Micro- and Nanostructure System Technology), Project 7.04 NOSE.

References

[1] J.K. Gimzewski, Ch. Gerber, E. Meyer, R.R. Schlittler, Chem. Phys. Lett. 217 (1994) 589.
[2] R. Berger, Ch. Gerber, J.K. Gimzewski, E. Meyer, H.-J. Güntherodt, Appl. Phys. Lett. 69 (1996) 40.
[3] Y. Nakagawa, R. Schäfer, Angew. Chem. Int. Ed. 38 (1999) 1083.

[4] T. Bachels, R. Schäfer, Chem. Phys. Lett. 300 (1999) 177.
[5] J.R. Barnes, R.J. Stephenson, M.E. Welland, Ch. Gerber, J.K. Gimzewski, Nature 372 (1994) 79.
[6] G.Y. Chen, T. Thundat, E.A. Wachter, R.J. Warmack, J. Appl. Phys. 77 (1995) 3618.
[7] R. Berger, Ch. Gerber, H.P. Lang, J.K. Gimzewski, Microelectron. Eng. 35 (1997) 373.
[8] R. Berger, E. Delamarche, H.P. Lang, Ch. Gerber, J.K. Gimzewski, E. Meyer, H.-J. Güntherodt, Science 276 (1997) 2021.
[9] T. Thundat, S.L. Sharp, W.G. Fisher, R.J. Warmack, E.A. Wachter, Appl. Phys. Lett. 66 (1995) 1563.
[10] T. Thundat, R.J. Warmack, G.Y. Chen, D.P. Allison, Appl. Phys. Lett. 64 (1994) 2894.
[11] T. Thundat, E.A. Wachter, S.L. Sharp, R.J. Warmack, Appl. Phys. Lett. 66 (1995) 1695.
[12] J. Lai, Z. Shi, T. Perazzo, A. Majumdar, Sensors Actuators 58 (1997) 113.
[13] J. Varesi, J. Lai, Z. Shi, T. Perazzo, A. Majumdar, Appl. Phys. Lett. 71 (1997) 306.
[14] T. Perazzo, M. Mao, O. Kwon, A. Majumdar, J.B. Varesi, P. Norton, Appl. Phys. Lett. 74 (1999) 3567.
[15] R. Berger, H.P. Lang, Ch. Gerber, J.K. Gimzewski, J.H. Fabian, L. Scandella, E. Meyer, H.-J. Güntherodt, Chem. Phys. Lett. 294 (1998) 363.
[16] H.-J. Butt, J. Colloid Interface Sci. 180 (1996) 251.
[17] H.P. Lang, R. Berger, C. Andreoli, J. Brugger, M. Despont, P. Vettiger, Ch. Gerber, J.K. Gimzewski, J.-P. Ramseyer, E. Meyer, H.-J. Güntherodt, Appl. Phys. Lett. 72 (1998) 383.
[18] H.P. Lang, R. Berger, C. Andreoli, J. Brugger, M. Despont, P. Vettiger, F. Battiston, J.-P. Ramseyer, E. Meyer, T. Mezzacasa, L. Scandella, H.-J. Güntherodt, Ch. Gerber, J.K. Gimzewski, Appl. Phys. A 66 (1998) S61.
[19] H.P. Lang, M.K. Baller, R. Berger, Ch. Gerber, J.K. Gimzewski, F.M. Battiston, P. Fornaro, J.P. Ramseyer, E. Meyer, H.-J. Güntherodt, Anal. Chim. Acta 393 (1999) 59.
[20] S.C. Minne, S.R. Manalis, C.F. Quate, Appl. Phys. Lett. 67 (1995) 3918.
[21] M.I. Lutwyche, Y. Wada, Sensors Actuators A 48 (1995) 127.
[22] S.A. Miller, K.L. Turner, N.C. McDonald, Proceedings of the Transducers '97, International Conference on Solid-State Sensors and Actuators, Chicago, June 16–19, 1997, IEEE, Piscataway, 1997, p. 455.
[23] W. Göpel, J. Hesse, J.N. Zemel (Eds.), Sensors: A Comprehensive Survey, Vols. 1–9, VCH, Weinheim, 1989–1996.
[24] H. Baltes, W. Göpel, J. Hesse (Eds.), Sensors Update, Vols. 1–5, VCH, Weinheim, 1996–1999.
[25] H.P. Lang, M. K. Baller, F.M. Battiston, J. Fritz, R. Berger, J.-P. Ramseyer, P. Fornaro, E. Meyer, H.-J. Güntherodt, J. Brugger, U. Drechsler, H. Rothuizen, M. Despont, P. Vettiger, Ch. Gerber, J.K. Gimzewski, Technical Digest 12th IEEE International Conference on Micro Electro Mechanical Systems "MEMS '99", Orlando, FL, USA, January 17–21, IEEE, Piscataway, 1999, p. 9.
[26] S. Prescesky, M. Parameswaran, A. Rawicz, R.F.B. Turner, U. Reichl, Can. J. Phys. 70 (1992) 1178.
[27] M.D. Antonik, N.P. D'Costa, J.H. Hoh, IEEE Eng. in Med. and Biol. (1997) 66.
[28] S.J. O'Shea, M.E. Welland, T.A. Brunt, A.R. Ramadan, T. Rayment, J. Vac. Sci. Technol. B 14 (1996) 1383.
[29] R. Raiteri, H.-J. Butt, J. Phys. Chem. 99 (1995) 15728.
[30] T. Thundat, P.I. Oden, R.J. Warmack, Microscale Thermophysical Engineering 1 (1997) 185.
[31] M. Zhang, T. Desai, M. Ferrari, Biomaterials 19 (1998) 953.